www.ThePharmaJournal.com

The Pharma Innovation

ISSN (E): 2277-7695
ISSN (P): 2349-8242
NAAS Rating: 5.23
TPI 2023; 12(12): 1007-1012

www.thepharmajournal.com
Received: 14-09-2023
Accepted: 23-10-2023

Mohit Panwar
Department of Chemistry, College of Basic Science and Humanities, G.B. Pant University of Agriculture and Technology, Pantnagar, Uttarakhand, India

Shweta Chand Thakuri
Department of Chemistry, College of Basic Science and Humanities, G.B. Pant University of Agriculture and Technology, Pantnagar, Uttarakhand, India

Vijay Kumar Juyal
Department of Chemistry, College of Basic Science and Humanities, G.B. Pant University of Agriculture and Technology, Pantnagar, Uttarakhand, India

Rashmi
Department of Chemistry, College of Basic Science and Humanities, G.B. Pant University of Agriculture and Technology, Pantnagar, Uttarakhand, India

Virendra Kasana
Department of Chemistry, College of Basic Science and Humanities, G.B. Pant University of Agriculture and Technology, Pantnagar, Uttarakhand, India

Viveka Nand
Department of Chemistry, College of Basic Science and Humanities, G.B. Pant University of Agriculture and Technology, Pantnagar, Uttarakhand, India

Corresponding Author:
Mohit Panwar
Department of Chemistry, College of Basic Science and Humanities, G.B. Pant University of Agriculture and Technology, Pantnagar, Uttarakhand, India

Thermal, spectroscopic, ADMET and toxicological studies of synthesized β-Amino carbonyl compounds

Mohit Panwar, Shweta Chand Thakuri, Vijay Kumar Juyal, Rashmi, Virendra Kasana and Viveka Nand

DOI: https://doi.org/10.22271/tpi.2023.v12.i12l.24593

Abstract
The β-amino carbonyl compound (C1), its–chloro (C2) and -methoxy (C3) derivatives were synthesized in this Mannich reaction type synthesis, wherein Guanine Hydrochloride was used as a catalyst. CHN elemental analyzer, UV-Vis, MS, FT-IR and NMR techniques, were used to characterize the compounds. The main objective of the study was to investigate the thermal behavior of these compounds, which was done by TGA/DTA/DTG analysis. The compounds were also tested for their toxicity and "drug-likeliness" as β-amino carbonyl compounds are generally well suited for pharmacological studies. Target compounds were achieved with 80-85% yield. All the compounds were decomposed at a temperature above 600 ºC, and showed non-spontaneous and endothermic reactions. The compounds did not show any abnormal behavior at higher temperature ranges. All the compounds were found to be less toxic and results were affirmative for their drug-likeliness based on Lipinski's rule of five. Hence, the nanostructures of these compounds, combined with heat stability, non-toxicity and drug-likeliness pave the way for their clinical assessment.

Keywords: Mannich Reaction, β-amino carbonyl, thermal behavior, nanostructures, drug-likeliness

1. Introduction
TGA has been used to investigate the thermal degradation kinetics and stability of ABS/SWNT composites and DSC to analyze their thermal properties, including phase transitions and crystallization behavior [1]. TGA also gives insights into the thermal behavior and decomposition kinetics of the polychelates [2]. Thermal studies have not been limited to this only. They have been utilized to study the solid-state reactions to study keto-enol tautomerism [3] and even to study the degradation of cellulose and hemicellulose in plants' extract [4].

Researchers have extensively studied β-amino carbonyl compounds for their antimicrobial property [5], anti-oxidant property [6], herbicidal property [7], and various other characteristics. Their therapeutic value holds significant importance [8], leading to their synthesis through various means and methods [9], aiming to reduce reaction time and enhance efficiency. These compounds have been found to exhibit inhibitory effects on specific metabolic enzymes [10] and play a crucial role in diverse heterocyclic synthesis and pharmaceutical development [11]. The oral bioavailability [12] and toxicity [13] assessments have indicated their promising potential as potent drugs. However, limited attention has been given to the investigation of the thermal properties of these compounds.

The need for finding the drug-like properties of a compound through its structure was long due in the allied sciences. Lipinksi devised a method, Rule of five (RO5) which predicts the oral drug-likeliness of the compounds based on the structure [14]. Depending on how it is administered, the term "drug-like" has a different connotation. The original RO5 focuses on orally active compounds and establishes four straightforward ranges of physicochemical parameters (MWT 500, log P 5, H-bond donors 5, H-bond acceptors 10) connected to 90% of orally active medications that have reached phase II clinical status. The initial stages in oral bioavailability are these physicochemical properties, which are linked to adequate aqueous solubility and intestinal permeability [15].

In the present scheme of work, β-amino carbonyl compounds were synthesized using a greener approach and the study focuses on the diffraction pattern and thermal analysis of the compounds formed. Information on phase transformation and volatile compound analysis was gathered by studying the behavior of these compounds in a Nitrogen environment at high

temperatures.
Furthermore, the assessment of toxicity and drug likeliness was done to validate the potential use of these compounds as potent drugs in pharmacological and medical applications.

2. Experimental

All chemicals used were of the analytical reagent grade and were used in their purest form available. The reagents for ligand, namely: benzaldehyde (assay>99%, Merck), aniline (assay>99%, Molychem), *p*-methoxy aniline (assay>99%, Molychem), *p*-chloroaniline (assay>99%, Molychem), acetophenone (assay>99%, HiMedia) were used. The catalyst used was Guanine Hydrochloride (assay>99%, HiMedia) and the medium of reaction was absolute ethanol (Merck).

2.1 Synthesis

A round-bottom flask was utilized as the reaction vessel for the synthesis. Benzaldehyde, acetophenone, and aniline were combined in stoichiometric proportions, and Guanine Hydrochloride was added as a catalyst. The reaction mixture was allowed to proceed until complete conversion was achieved and TLC constantly monitored the reaction progress. To remove impurities, the reaction mixture was washed with distilled water. The resulting crude product was obtained after the washing process. The crude product (C1) was further purified by recrystallization. The same process described above was repeated for other derivatives but with different reagents. In this case, *p*-chloroaniline (product C2) and *p*-methoxy aniline (product C3) were used instead of aniline. Scheme 1-3 represents the target synthesis products.

2.1.1 $C_{21}H_{19}NO$ (C1)

Yield 85%; Colour: buff; M.pt. 133 ℃;1H NMR (400 MHz, DMSO-D6) δ 7.76 – 7.61 (m, 2H), 7.44 – 7.31 (m, 1H), 7.35 – 7.18 (m, 4H), 7.04 (dd, J = 8.3, 6.9 Hz, 2H), 6.98 – 6.89 (m, 1H), 6.77 – 6.68 (m, 2H), 6.29 – 6.17 (m, 2H), 5.98 (d, J = 7.7 Hz, 1H), 4.75 (td, J = 8.3, 4.5 Hz, 1H), 3.39 (dd, J = 17.0, 8.9 Hz, 1H), 3.13 – 2.99 (m, 2H);13C NMR (101 MHz, DMSO-D6) δ 202.63, 153.13, 149.37, 142.10, 138.49, 134.01, 133.62, 133.36, 132.02, 131.95, 121.10, 118.12, 58.13, 51.76, 45.43, 45.23, 45.02, 44.81, 44.60, 44.39, 44.18.FTIR: 3372; 1662(s); 1287 (s); 900-1100 cm^{-1}.

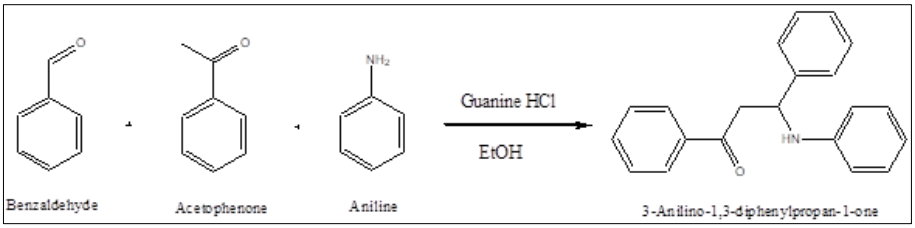

Scheme 1: Synthesis of 1, 3-diphenyl-3-(phenyl amino) propan-1-one

2.1.2 $C_{21}H_{18}ClNO$ (C2): Yield 85%; Colour: cream; M.pt. 156 ℃; 1H NMR (400 MHz, DMSO-D6) δ 7.93 (dt, J = 7.1, 1.4 Hz, 2H), 7.64 – 7.54 (m, 1H), 7.48 (t, J = 7.6 Hz, 2H), 7.47 – 7.38 (m, 2H), 7.26 (t, J = 7.6 Hz, 2H), 7.20 – 7.11 (m, 1H), 7.01 – 6.92 (m, 2H), 6.51 – 6.39 (m, 3H), 4.94 (td, J = 8.3, 4.4 Hz, 1H), 3.60 (dd, J = 17.1, 8.9 Hz, 1H), 3.36 – 3.23 (m, 1H);13C NMR (101 MHz, DMSO-D6) δ 197.67, 147.31, 144.14, 137.25, 133.76, 129.82, 129.25, 129.12, 128.97, 128.93, 128.60, 127.38, 127.16, 119.62, 114.68, 53.39, 46.92. FTIR: 3376; 1659 (sh); 1280 (sh); 900-1100; 738 cm^{-1}.

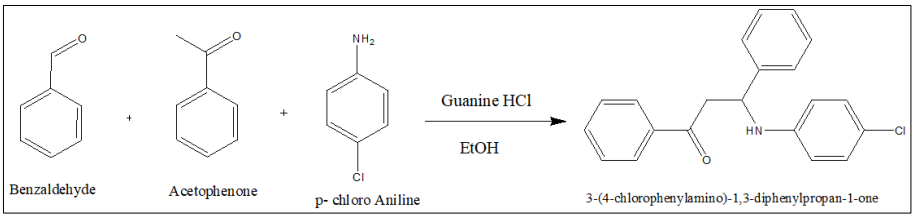

Scheme 2: Synthesis of 3-(4-chlorophenylamino)-1,3-diphenylpropan-1-one

2.1.3 $C_{22}H_{21}NO_2$ (C3): Yield 85%; Colour: Dark grey; M.pt. 106 ℃; 1H NMR (400 MHz, DMSO-D6) δ 8.60 (s, 1H), 7.97 – 7.83 (m, 3H), 7.52 – 7.42 (m, 5H), 7.46 – 7.37 (m, 0H), 7.31 – 7.20 (m, 3H), 6.99 – 6.90 (m, 3H), 6.62 – 6.53 (m, 1H), 6.46 – 6.38 (m, 1H), 4.86(s,1H), 3.74 (s, 3H), 3.53 (s, 1H), 3.34 (s,1H); 13C NMR (101 MHz, DMSO-D6) δ 198.08, 158.88, 158.50, 151.25, 144.76, 144.61, 142.50, 137.38, 136.84, 133.69, 131.61, 129.32, 129.23, 128.94, 128.80, 128.60, 127.25, 122.97, 114.94, 114.55, 55.83, 55.71, 54.33, 47.09. FTIR: 3373; 1666(s); 1279 (s); 900-1100; 1027cm^{-1}.

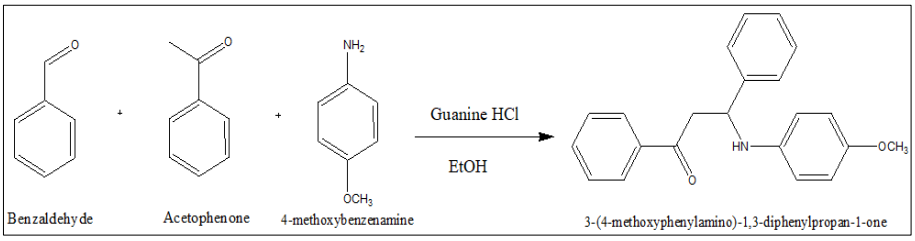

Scheme 3: Synthesis of 3-(4-methoxyphenylamino)-1,3-diphenylpropan-1-one.

2.2 Physical and Spectral Measurement

The compound's properties were characterized using various analytical techniques. The melting point was determined using the Decibel DB-3135H melting point apparatus. Molar conductivity was measured with the Systronic conductivity TDS meter 308. Elemental analysis for carbon, hydrogen, and nitrogen (C, H, N) was performed using the Elementar Analysensysteme Germany (Vario Micro Cube). The ^{1}H-NMR and ^{13}C-NMR spectra were recorded using the Jeol JNM-ECZ 400S instrument operating at 400 MHz and 100 MHz, respectively. The molecular weight was determined via Mass Spectrometry using the Xevo G2-XS QTof Mass Spectrophotometer, while FTIR (ATR) analysis was conducted using the Nicolet iS50 FTIR Tri-detector.

2.3 Thermal studies

Thermal Gravimetric Analysis (TGA), Differential Thermal Analysis (DTA) and Differential Thermal Gravimetric analysis (DTG) curve of ligands (C1, C2, and C3) were obtained in an N_2 environment in an EXSTAR TG/DTA 6300 instrument with a heating rate of 10^0C/min. The experimental temperature range between 25–1000°C was used to study the thermal stability.

2.4 ADMET and Toxicology Studies

Virtual screening was conducted to analyze the physicochemical properties and evaluate the pharmacokinetics (drug-likeliness) of the selected compounds using the SwissADME tool [16-17], whereas PROTOX-II software was used to find the oral toxicity and bioavailability [18]. ChemDraw software was used to generate the SMILES format required for SwissADME and PROTOX-II [19].

3. Results and Discussion

3.1 IR Spectral Data

The FT-IR spectra of the samples were recorded after completely dehydrating the samples in a hot air oven, to avoid any water molecule peaks. The spectra represented in Fig. 1 shows the FTIR spectra of the compounds.

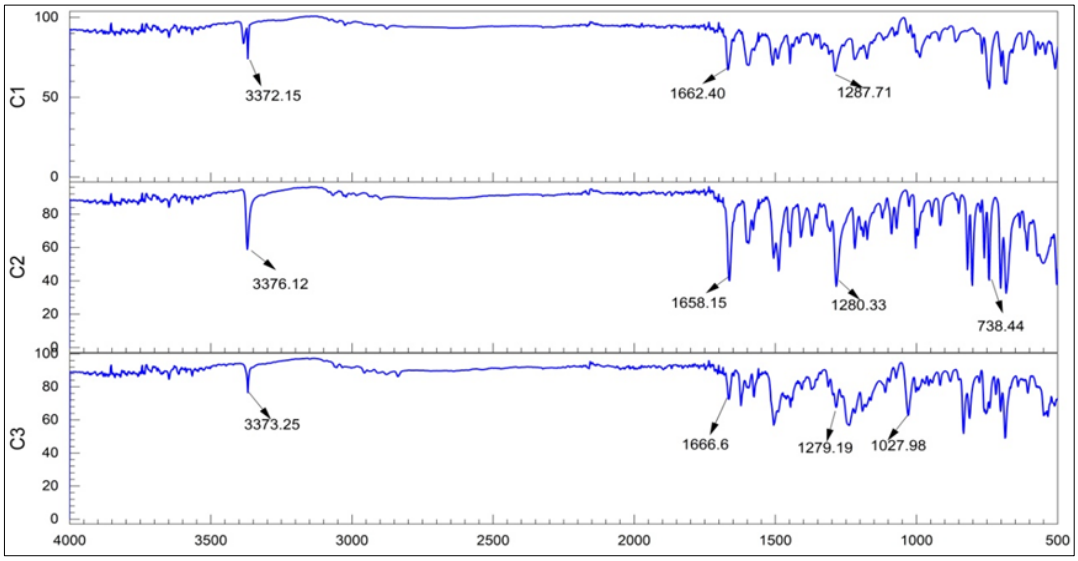

Fig 1: FT-IR spectra of synthesized compounds.

All three compounds (C1, C2, C3) show N-H characteristic stretching at around 3375 cm^{-1} and C=O stretching at around 1660 cm^{-1}. This shows the presence of both amine and carbonyl groups in all three, with little difference. This difference could be due to amine group substitution, which is observed at 738 cm^{-1} (C-Cl stretch) and 1027cm^{-1}(C-O-C stretch) in the case of C2 & C3 respectively. Thus, the spectra confirm the formation ofan amine group and a ketone group in all three, while C-Cl and C-OCH$_3$ in C2 and C3, respectively.

3.2 NMR Analysis

All the synthesized compounds showed striking similarity with expected ^{1}H and ^{13}C spectra. In 13C spectra, all of the compounds showed a carbonyl range between 197-202 ppm, confirming keto-bond. In 1H spectra, the range between 4.95-4.75 ppm and 3.39-3.60 ppm corresponds to β and α carbon (next to the carbonyl group) respectively. The values between 3.13 - 3.36 ppm correspond to the N-H stretch. Hence, all the compounds are β-amino ketone derivatives. Moreover, the chemical shift of 3.34 (s, 3H) is characteristic of the O-CH$_3$bond, which is observed for C3 (a methoxy derivative).

3.3 UV-Vis Spectral Analysis

Different values clearly represent the formation of three different compounds with a bathochromic shift with the increase in substituent group. Table 1 presents the elemental composition, showing a remarkable resemblance between the calculated and found values.

Table 1: CHN Elemental Analysis data and UV-Vis Spectral values

Compound	C	H	N	π-π^*	n-π^*
C1	84.71(83.69)	5.28(6.35)	5.54(4.65)	265	370
C2	74.79(75.11)	5.226(5.4)	4.97(4.17)	275	355
C3	78.82(79.73)	6.134(6.39)	4.67(4.236)	335	385

3.4 Thermal Analysis (TGA, DTA and DTG analysis)

The TG/DTG/DTA curves of ligands C1, C2, and C3 show two to three steps decomposition profiles and demonstrate a similar behavior in thermal stability.

In the case of ligand C1, a three-step decomposition pattern (3 DTA peaks) was seen in which the initial weight loss starts at ~29 ℃ associated with a lossin mass of about 0.30% due removal of adsorbed water molecules on the surface of the

ligand. In the second stage, onset starts at ~100 ℃ associated with a loss in mass of about 28.10% w.r.t initial weight due to the phase transformation of the ligand (as seen in XRD pattern of C1) [20]. A sharp degradation starts at ~ 200 ℃ with a weight loss of 90.80% w.r.t initial weight due to the decomposition of ligands [21]. The stable product was obtained at ~300 ℃. The DTG peaks showing a maximum rate of mass loss corresponding to the above changes were observed at 156 ℃ and 274 ℃, corresponding to phase transformations [22]. TGAcurve shows endothermic peaks at 58 ℃, 133 ℃ and 278 ℃ due to dehydration, phase transformation, and degradation of ligand moiety and this can be correlated with thermodynamics parameters (ΔH, ΔG) calculated using TGA data [23]. The activation energy calculated for first, second and third steps of reaction are 36.17 kJ mol^{-1}, 72.59 kJ mol^{-1} and 52.07 kJ mol^{-1} respectively.

In the case of ligand C2, a two-step decomposition pattern was seen in which weight loss of about 29.80% w.r.t initial weight is observed due to phase transformation starts at ~ 100 ℃. A sharp degradation starts at ~ 200 ℃ with a weight loss of 96.70% w.r.t initial weight due to the decomposition of ligand and the stable product is obtained at ~300 ℃. The maximum rate of mass loss from DTG peaks corresponding to the above changes were observed at 192 ℃ and 272 ℃. The DTA curve in all the steps shows endothermic peaks at 150 ℃ and 276 ℃ due to phase transformation and degradation of ligand moiety and this can be correlated with thermodynamic parameters (ΔH, ΔG) calculated using TGA data. The activation energy calculated for first and second steps of the reaction are 60.80 kJ mol^{-1} and 54.40 kJ mol^{-1} respectively.

In the C3ligand, a three-step decomposition pattern was observed in which the initial weight loss starts at ~33 ℃ associated with a loss in minute mass of about 0.30% w.r.t initial weight due to evaporation and dehydration. In step 2, weight loss starts at ~100 ℃ associated with a loss in mass of about 16.70% w.r.t initial weight due to phase transformation of the ligand. In step 3, and a sharp degradation starts at ~ 200 ℃ with a weight loss of 90.70% w.r.t initial weight due to the decomposition of ligand moiety and the stable product is obtained at ~285 ℃. The DTG peak showing a maximum rate of mass loss corresponding to the above changes was observed at 274 ℃. The DTA curve in all the steps showing weight loss, as identified in TGA curve shows endothermic peaks at 73 ℃, 106 ℃ and 276 ℃ due to dehydration, phase transformation and degradation of ligand moiety and this can be correlated with thermodynamics parameters (ΔH, ΔG) calculated using TGA data. The activation energy calculated for the first, second and third step of the reaction are 40.49 KJ mol^{-1}, 69.42 KJ mol^{-1}, and 66.66 KJ mol^{-1} respectively. Fig. 2 represents TGA/DTA/DTG analyses of the compounds C1, C2 and C3.

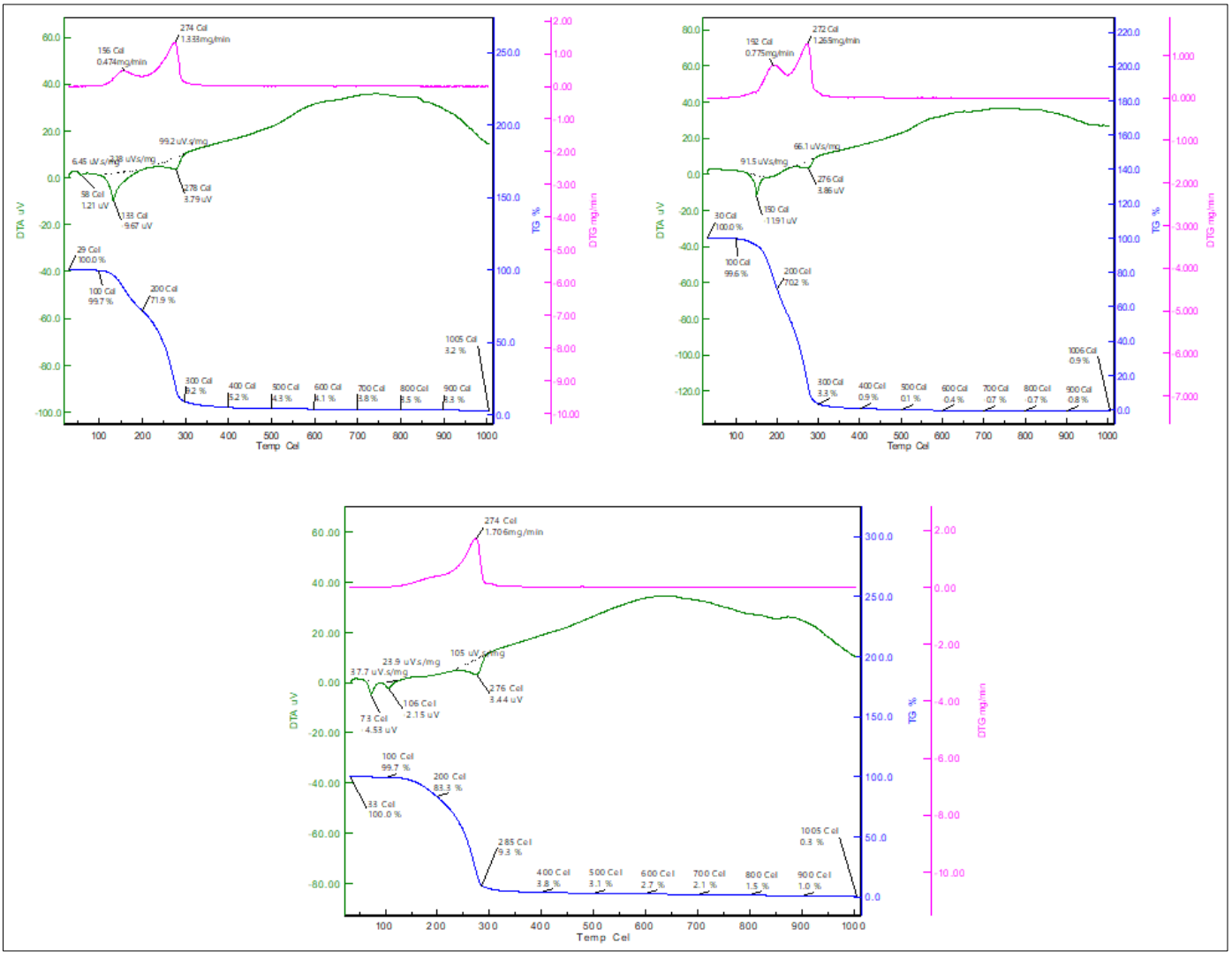

Fig 2: TGA/DTA/DTG analyses of the compounds C1, C2 and C3.

Considering all phase transformations as 1st order reactions [24], activation energy, change in enthalpy, spontaneity, and Gibbs free energy were determined using 1st order reaction rate equation as given in Eq. 1

$$\frac{dx}{dt} = k(1-x) \quad (1)$$

Where, $x=\frac{wi-wt}{wi-wf}$

w_i, w_t and w_f represents the initial weight, weight of the sample at a particular time t, and final weight respectively. Eq. 1 can be rewritten as

$$\ln(1-x) = -kt \quad (2)$$

Data were plotted using Eq. 2 and the straight line was followed for each phase, proving that transformations were first-order reactions [25]. The slope of each line provided the rate constant (k) value for a certain step, and Eq. 3 was used to calculate the half-life ($t_{1/2}$).

$$t_{1/2} = \frac{0.693}{k} \quad (3)$$

Table 2: Kinetic and thermodynamic parameters of each phase during TGA

S. No	ligand	Number of steps	Temp. (ºC)	Temp. (K)	K (min^1)	$T_{1/2}$ (min)	E_a ($KJmol^{-1}$)	ΔH ($KJmol^{-1}$)	ΔS ($KJmol^{-1}$ K^{-1})	ΔG ($KJmol^{-1}$
1	C1	Step 1	100	373	0.3791	1.82	36.17	33.06	-245.55	12.46
		Step 2	200	473	0.0803	8.63	72.59	68.65	-140.81	13.52
		Step 3	300	573	0.0446	15.53	52.07	47.30	-199.38	16.15
2.	C2	Step 1	200	473	0.1667	4.15	60.80	56.87	-174.03	13.91
		Step 2	300	573	0.0445	15.57	54.40	49.64	-192.78	16.01
3.	C3	Step 1	100	373	0.0003	231	40.49	37.39	-231.05	12.35
		Step 2	200	473	0.0169	41	69.42	65.49	-156.63	13.95
		Step 3	285	558	0.2219	3.12	66.66	62.02	-170.63	15.72

Kinetics parameters were determined using a modified form of Coats and Redfern model [26] as described in Eq. 4

$$\ln[-\ln(1-x)] = ln\frac{ART^2}{\beta Ea} - \frac{E_a}{RT} \quad (4)$$

Where A is the pre-exponential factor, β is the heating rate (10 ℃/min), R is the universal gas constant (8.3143 $Jmol^{-1}$ K^{-1}), E_a is activation energy and T is the temperature (K). The activation energy for each phase was estimated by plotting graphs between ln[-ln(1-x)] versus 1000/T, and further parameters were calculated using fundamental thermodynamic equations [27]. Table 2 represents the values obtained for each phase and shows that all phases undergo non-spontaneous endothermic changes with an increase in temperature.

3.5 ADMET and toxicity studies: The compounds underwent *in-silico* ADME and toxicity studies, revealing their moderate toxicity and classification into class 4 toxicity, as detailed in Table 3. Furthermore, the compounds were deemed favorable in terms of drug-likeness, complying with Lipinski's rule of five, thereby demonstrating their potential for effective utilization in pharmaceutical applications.

Table 3: *In-silico* ADME and toxicity studies of the compounds

Compound	M. Wt	H-bond donors	H-bond acceptors	Log P	Drug-Likeliness	LD50	Toxicity Class
C1	301.38	1	1	4.04	Yes	1600	4
C2	335.83	1	1	4.53	Yes	500	4
C3	331.41	1	2	3.65	Yes	1500	4

4. Conclusion

The synthesis of a β-amino carbonyl compound (C1) and its –chloro (C2) and -methoxy (C3) derivatives was successfully revealed and characterized using a range of spectroscopic and analytical techniques. Thermal analysis of the compounds demonstrated their decomposition, phase transformation, and stability across various temperature ranges. These findings indicate the potential of these compounds as drug-like molecules, possessing nano size and heat stability, which holds promising applications in diverse pharmacological and medical fields, highlighting their potency and value for future research and development.

5. Acknowledgement

The author is thankful to G.B Pant University of agriculture and technology for providing research facilities. The author acknowledges CRF IIT Ropar for MS characterization, IIC IIT Roorkee for TGA characterization, and USIC Delhi University for C, H, N analysis, NMR analysis and FTIR analysis.

6. References

1. Yang S, Castilleja JR, Barrera EV, Lozano K. Thermal analysis of an acrylonitrile–butadiene–styrene/SWNT composite. Polymer Degradation and Stability. 2004;83(3):383-388. https://doi.org/10.1016/j.polymdegradstab.2003.08.002.
2. Chikate RC, Bajaj HA, Kumbhar AS, Kolhe VC, Padhye SB. Thermal and spectral properties of lanthanide (III) complexes of 3-amino-2-hydroxy-1,4-naphthoquinone. Thermochimica Acta. 1995;249:239-248. https://doi.org/10.1016/0040-6031(95)90702-5.
3. El-Boraey HA. Structural and thermal studies of some aroylhydrazone Schiff's bases-transition metal complexes. Journal of Thermal Analysis and Calorimetry. 2005;81:339-346. https://doi.org/10.1007/s10973-005-0789-0.
4. Ram VR, Ram PN, Khatri TT, Vyas SJ, Dave PN. Thermal analytical characteristics by TGA-DTA-DSC analysis of *Carica papaya* leaves from Kachchh. International Letters of Natural Sciences. 2014;(21).

5. Fuh MT, Tseng CC, Li SM, Tsai SE, Chuang TJ, Lu CH, et al. Design, synthesis and biological evaluation of glycolamide, glycinamide, and β-amino carbonyl 1, 2, 4-triazole derivatives as DPP-4 inhibitors. Bioorganic Chemistry. 2021;114:105049. http://doi.org/10.1016/j.bioorg.2021.105049.
6. Kenchappa R, Bodke YD, Peethambar SK, Telkar S, Bhovi VK. Synthesis of β-amino carbonyl derivatives of coumarin and benzofuran and evaluation of their biological activity. Medicinal Chemistry Research. 2013;22:4787-4797. http://doi.org/10.1007/s00044-013-0494-7.
7. Bhandari S, Agrwal A, Kasana V, Tandon S, Boulaamane Y, Maurady A. β-amino carbonyl derivatives: Synthesis, Molecular Docking, ADMET, Molecular Dynamic and Herbicidal studies. ChemistrySelect. 2022;7(48):e202201572. http://doi.org/10.1002/slct.202201572.
8. Zhang ZY, Zhu YH, Zhou CH, Liu Q, Lu HL, Ge YJ, et al. Development of β-amino-carbonyl compounds as androgen receptor antagonists. Acta Pharmacologica Sinica. 2014;35(5):664-673. http://doi.org/10.1038/aps.2013.201.
9. Weiner B, Szymański W, Janssen DB, Minnaard AJ, Feringa BL. Recent advances in the catalytic asymmetric synthesis of β-amino acids. Chemical Society Reviews. 2010;39(5):1656-1691. http://doi.org/10.1039/B919599H.
10. Biçer R, Kaya G, Yakalı MS, Gültekin GT, Cin İ. Gülçin. Synthesis of novel β-amino carbonyl derivatives and their inhibition effects on some metabolic enzymes. Journal of Molecular Structure. 2020;1204:127453. http://doi.org/10.1016/j.molstruc.2019.127453.
11. Govindh, Diwakar BS, Murthy YL. A brief review on synthesis & applications of [beta]-enamino carbonyl compounds. Organic Communications. 2012;5(3):105.
12. Nidhar M, Kumar V, Mahapatra A, Gupta P, Yadav P, Sonker P, et al. Lead modification via computational studies: Synthesis of pyrazole-containing β-amino carbonyls for the treatment of type 2 diabetes. Chemical Biology & Drug Design. 2023;101(3):638-649. http://doi.org/10.1111/cbdd.14157.
13. Nidhar M, Kumar V, Mahapatra A, Gupta P, Yadav P, Sonker P, et al. Lead modification via computational studies: Synthesis of pyrazole-containing β-amino carbonyls for the treatment of type 2 diabetes. Chemical Biology & Drug Design. 2023;101(3):638-649.
14. Pollastri MP. Overview on the Rule of Five. Current Protocols in Pharmacology. 2010;49(1):9-12.
15. Lipinski CA. Lead-and drug-like compounds: the rule-of-five revolution. Drug Discovery Today: Technologies. 2004;1(4):337-341.
16. Šestić TL, Ajduković JJ, Marinović MA, Petri ET, Savić MP. In silico ADMET analysis of the A-, B-and D-modified androstane derivatives with potential anticancer effects. Steroids. 2023;189:109147. Available from: http://doi.org/10.1016/j.steroids.2022.109147.
17. Daina A, Michielin O, Zoete V. SwissADME: A free web tool to evaluate pharmacokinetics, drug-likeness and medicinal chemistry friendliness of small molecules. Scientific Reports. 2017;7(1):42717. Available from: http://doi.org/10.1038/srep42717.
18. Banerjee P, Eckert AO, Schrey AK, Preissner R. ProTox-II: a webserver for the prediction of toxicity of chemicals. Nucleic Acids Research. 2018;46(W1):W257-W263. Available from: http://doi.org/10.1093/nar/gky318.
19. Abdullahi M, Adeniji SE. In-silico molecular docking and ADME/pharmacokinetic prediction studies of some novel carboxamide derivatives as anti-tubercular agents. Chemistry Africa. 2020;3(4):989-1000.
20. Wang S, Gainey L, Baxter D, Wang X, Mackinnon ID, Xi Y. Thermal behaviours of clay mixtures during brick firing: A combined study of in-situ XRD, TGA and thermal dilatometry. Construction and Building Materials. 2023;299:124319.
21. Chen Z, Wu Y, Huang F, Gu D, Gan F. Synthesis, spectral, and thermal characterizations of Ni (II) and Cu (II) β-diketone complexes with thenoyltrifluoroacetone ligand. Spectrochimica Acta Part A: Molecular and Biomolecular Spectroscopy. 2007;66(4-5):1024-1029. Available from: http://doi.org/10.1016/j.saa.2006.05.015.
22. Joshi S, Srivastava RK. Characterization and synthesis of chitosan-silica gel and chitosan-bentonite composites for adsorption of heavy metals. Nature Environment and Pollution Technology. 2016;15(4):1237.
23. Farrukh MA, Butt KM, Chong KK, Chang WS. Photoluminescence emission behavior on the reduced band gap of Fe doping in CeO2-SiO2 nanocomposite and photophysical properties. Journal of Saudi Chemical Society. 2019;23(5):561-575. Available from: http://doi.org/10.1016/j.jscs.2018.10.002.
24. Perveen S, Farrukh MA. Influence of lanthanum precursors on the heterogeneous La/SnO 2–TiO 2 nanocatalyst with enhanced catalytic activity under visible light. Journal of Materials Science: Materials in Electronics. 2017;28:10806-10818. Available from: http://doi.org/10.1007/s10854-017-6858-x.
25. Zhang B, Zhu T, Ou M, Rowell N, Fan H, Han J, et al. Thermally-induced reversible structural isomerization in colloidal semiconductor CdS magic-size clusters. Nature Communications. 2018;9(1):2499. Available from: http://doi.org/10.1038/s41467-018-04842-0.
26. Ramukutty S, Ramachandran E. Reaction rate models for the thermal decomposition of ibuprofen crystals. Journal of Crystallization Process and Technology. 2014.
27. del Mar Graciani M, Rodríguez A, Muñoz M, Moyá ML. Micellar Solutions of Sulfobetaine Surfactants in Water− Ethylene Glycol Mixtures: Surface tension, fluorescence, spectroscopic, conductometric, and kinetic studies. Langmuir. 2005;21(16):7161-7169. Available from: http://doi.org/10.1021/la050862j.